FEBS Letters 586 (2012) 4173–4179

journal homepage: www.FEBSLetters.org

Ligand binding and conformational states of the photoprotein obelin

Elena V. Eremeeva [a,b,c], Eugene S. Vysotski [a,b], Adrie H. Westphal [c], Carlo P.M. van Mierlo [c], Willem J.H. van Berkel [c,*]

[a] Photobiology Laboratory, Institute of Biophysics, Russian Academy of Sciences, Siberian Branch, Krasnoyarsk 660036, Russia
[b] Laboratory of Bioluminescence Biotechnology, Institute of Fundamental Biology and Biotechnology, Siberian Federal University, Krasnoyarsk 660041, Russia
[c] Laboratory of Biochemistry, Wageningen University, 6703 HA Wageningen, The Netherlands

ARTICLE INFO

Article history:
Received 24 August 2012
Revised 5 October 2012
Accepted 5 October 2012
Available online 23 October 2012

Edited by Richard Cogdell

Keywords:
Bioluminescence
Coelenterazine
Photoprotein
Thermostability

ABSTRACT

Many proteins require a non-covalently bound ligand to be functional. How ligand binding affects protein conformation is often unknown. Here we address thermal unfolding of the free and ligand-bound forms of photoprotein obelin. Fluorescence and far-UV circular dichroism (CD) data show that the various ligand-dependent conformational states of obelin differ significantly in stability against thermal unfolding. Binding of coelenterazine and calcium considerably stabilizes obelin. In solution, all obelin structures are similar, except for apo-obelin without calcium. This latter protein is an ensemble of conformational states, the populations of which alter upon increasing temperature.

1. Introduction

Many proteins require binding of a ligand to be functional. These ligands vary in size and complexity from a single metal ion to large organic molecules. Ligand binding can influence protein structure in different ways. For example, apocytochrome *c* is largely unstructured but upon incorporation of heme it turns into a well-ordered helical protein [1]. In contrast, apoflavodoxin is structurally identical to holoflavodoxin, except for increased dynamics [2–4].

Ca^{2+}-regulated photoproteins responsible for bioluminescence of various coelenterates consist of a single polypeptide chain of about 22 kDa. The substrate of the photoprotein bioluminescence reaction, coelenterazine, is widely distributed in luminous and non-luminous marine organisms, and has been identified as a luciferin in various luminous organisms [5]. Recombinant apo-photoproteins are converted to their active 2-hydroperoxycoelenterazine-liganded forms upon incubation under calcium-free conditions with coelenterazine in presence of oxygen and thiol-reducing agents [6].

Photoproteins contain three canonic EF-hand Ca^{2+}-binding sites. Calcium binding initiates oxidative decarboxylation of 2-hydroperoxycoelenterazine, resulting in the excited state of the product, coelenteramide [7], which relaxes to its ground state by emitting blue light with, depending on the type of photoprotein involved, emission maxima of 465–495 nm [8]. Coelenteramide remains bound after the bioluminescence reaction and the resulting protein–ligand complex is generally referred to as "Ca^{2+}-discharged photoprotein". Without calcium, photoproteins display a very low level of light emission called "calcium-independent luminescence" [9]. Upon calcium binding light intensity increases by six orders of magnitude or more.

Photoprotein obelin populates five conformational states (Fig. 1): apo-protein (I), active photoprotein with 2-hydroperoxycoelenterazine (II), Ca^{2+}-discharged photoprotein containing coelenteramide and calcium (III), Ca^{2+}-discharged photoprotein containing only coelenteramide (IV), and apo-protein containing calcium ions (V) [10]. To date the spatial structures of four conformational states (II, III, IV, and V) have been determined by X-ray crystallography [11].

In this paper, we report the effects ligands have on conformational states of obelin by using fluorescence and far-UV CD spectroscopy. We demonstrate that the binding of these ligands considerably stabilizes obelin against thermal unfolding. Apo-obelin containing no ligand (I) turns out to be an ensemble of conformational states and it is the least stable obelin conformation.

2. Materials and methods

2.1. Chemicals

Coelenterazine was obtained from Prolume Ltd. (Pinetop, USA). Other chemicals were obtained at the purest grade available from Sigma–Aldrich, unless mentioned otherwise.

* Corresponding author. Fax: +31 317 484801.
E-mail address: willem.vanberkel@wur.nl (W.J.H. van Berkel).

0014-5793/$36.00
http://dx.doi.org/10.1016/j.febslet.2012.10.015

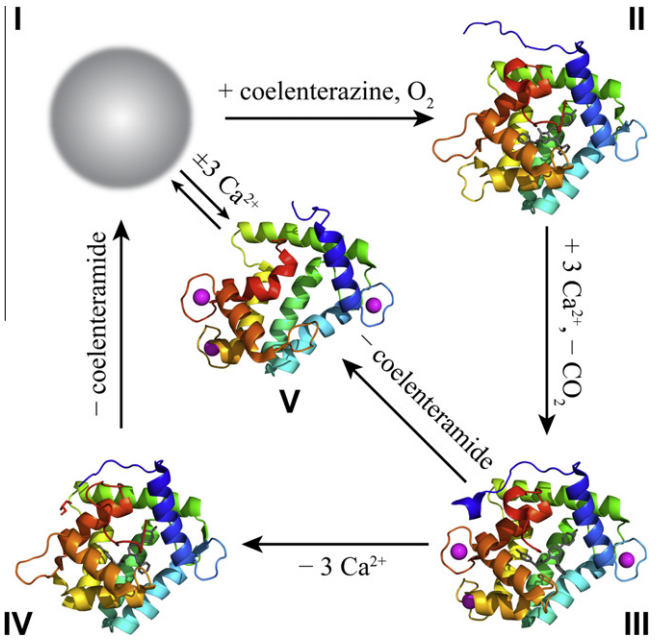

Fig. 1. Conformational states of obelin. (I) apo-obelin; (II) active obelin containing 2-hydroperoxycoelenterazine (PDB ID code 1EL4); (III) Ca^{2+}-discharged obelin containing both coelenteramide and calcium (PDB ID code 2F8P); (IV) Ca^{2+}-discharged obelin containing coelenteramide (PDB ID code 1S36); (V) calcium-loaded apo-obelin (PDB ID code 1SL7). The structure of apo-obelin is unknown. 2-hydroperoxycoelenterazine and coelenteramide are displayed in stick representation; calcium ions are shown as magenta balls.

2.2. Protein expression and purification

Recombinant apo-obelin was expressed as reported [12,13]. For protein production, transformed *Escherichia coli* BL21-Gold was cultivated under vigorous shaking at 37 °C in LB medium containing 200 μg/ml ampicillin. Induction was initiated by adding 0.5 mM IPTG once the culture reached an OD600 of 0.5–0.6, and cultivation continued for another 3 h. Apo-obelin predominantly accumulated as inclusion bodies.

Apo-obelin (I) was purified from inclusion bodies as described [12,13] and concentrated by using Amicon Ultra Centrifugal Filters (Millipore). To fold apo-obelin, concentrated protein samples in 6 M urea were diluted approximately 20-fold with buffer, which contains 1 mM EDTA and 20 mM Tris–HCl, pH 7.0. Subsequently, the protein was concentrated, diluted, and concentrated again. This washing procedure was repeated several times to remove all urea and excess salt. Next, apo-obelin was passed through a Superdex 200 column (Amersham Bioscience) equilibrated with 5 mM EDTA, 20 mM Tris–HCl, pH 7.0 to produce monomeric apo-photoprotein.

Active obelin containing 2-hydroperoxycoelenterazine (II) was produced as reported [12,13]. To prepare Ca^{2+}-discharged obelin with coelenteramide and calcium bound (III), active obelin was diluted in 1 mM $CaCl_2$, 20 mM Tris–HCl, pH 7.0. After bioluminescence ceased, the sample was concentrated and passed through a Bio Gel P2 column equilibrated with 1 mM $CaCl_2$, 20 mM Tris–HCl, pH 7.0. Ca^{2+}-discharged obelin containing only coelenteramide (IV) was produced by addition of 5 mM EDTA to obelin conformation state (III) and passing through the same column but now equilibrated with 5 mM EDTA, 20 mM Tris–HCl, pH 7.0. All obelin samples were of high purity according to 12.5% SDS–PAGE.

Coelenterazine concentration was determined by measuring absorbance at 435 nm, using a molar absorption coefficient of 9800 M^{-1} cm^{-1} [5]. Concentrations of apo-obelin and obelin were determined by measuring absorbances at 280 nm, using molar absorption coefficients of 40450 M^{-1} cm^{-1} and 55500 M^{-1} cm^{-1}, respectively [14].

2.3. Fluorescence spectroscopy

Obelin fluorescence was measured at 20 °C with a Varian Cary Eclipse spectrofluorimeter. Excitation was set at 295 nm and emission was recorded between 305 and 550 nm at 1 nm intervals with a scan rate of 600 nm min^{-1} and 0.1 s averaging time.

Protein thermal unfolding was followed by recording fluorescence emission at 330, 340 and 350 nm, respectively. Temperature was increased at a rate of 1 °C/min from 16 to 80 °C in a 1.5 ml stirred quartz cuvette (path length 0.4 cm). Cooling down was achieved with a rate of 1 °C/min. In all fluorescence experiments, excitation and emission slits were set to a width of 5 nm. Protein concentration was 1.2 μM in 25 mM HEPES, pH 7.0, containing either 1 mM EDTA or 1 mM $CaCl_2$.

2.4. Far-UV CD

Far-UV CD spectra of ligand-dependent obelin conformations were recorded with a Jasco J-715 spectropolarimeter (Tokyo, Japan) equipped with a PTC-348WI Peltier temperature control system. Thermal unfolding of ligand-dependent obelin conformations was followed at 220 nm. Temperature was increased from 12 to 80 °C at a rate of 1 °C/min in a 1 mL stirred quartz cuvette (path length 0.1 cm). Protein concentration was 4 μM in 25 mM HEPES, pH 7.0, containing either 1 mM EDTA or 1 mM $CaCl_2$. Before and after thermal unfolding, far-UV CD spectra were recorded at 20 °C by averaging 20 scans. Sample spectra were corrected by subtracting spectra of corresponding blank solutions.

2.5. Data analysis

Thermal unfolding data were fitted to a two-state mechanism of unfolding, in which only the native and denatured states are populated. The change in free energy for thermal-induced protein unfolding, $\Delta G(T)$, is described by the modified Gibbs–Helmholtz equation:

$$\Delta G(T) = \Delta H_m(1 - T/T_m) - \Delta C_p[(T_m - T) + T\ln(T/T_m)] \quad (1)$$

where ΔH_m is the enthalpy change for unfolding measured at T_m, T the absolute temperature, T_m, the temperature at the midpoint of transition, and ΔC_p is the difference in heat capacity between unfolded and folded states [15,16]. Under the assumption that ΔC_p is temperature independent [17], a two-state mechanism of unfolding can be fitted to individual thermal unfolding curves:

$$Y_{obs} = (a_U + b_U T) + \frac{((a_N + b_N T) - (a_U + b_U T))}{(1 + \exp(((-\Delta H_m/R)(1/T - 1/T_m)) + ((\Delta C_p/R)(((T_m/T) - 1) + \ln(T/T_m)))))} \quad (2)$$

where Y_{obs} is the measured far-UV CD or fluorescence signal, R the gas constant, and a and b the intercepts and slopes of pre- and post-unfolding baselines that linearly depend on temperature, respectively. Eq. (2) was fitted to the thermal unfolding data by using the non-linear least-squares algorithm provided in the Microsoft Excel package. While fitting the thermal unfolding data obtained by both CD and fluorescence, ΔC_p was used as an adjustable parameter. Data shown present repetitive studies carried out on independently produced and purified protein samples.

3. Results

3.1. Thermal unfolding of obelin studied by fluorescence

Tryptophan fluorescence of apo-obelin (I) has a maximum at 340 nm [14]. Upon denaturant-induced unfolding of apo-obelin with 6.0 M GuHCl, the emission maximum shifts to 350 nm while

fluorescence intensity slightly increases (Fig. 2). Upon heat-induced unfolding of apo-obelin (I) by increasing temperature to 80 °C and subsequent cooling down to 20 °C, fluorescence intensity of refolded protein has its maximum at 343 nm and has 17% reduction of fluorescence intensity as compared to starting material (Fig. 2). This observation suggests that thermal unfolding of apo-obelin (I) is not fully reversible. Reversibility of thermal unfolding of apo-obelin loaded with calcium (V, Fig. 1) is less efficient (up to 50% reduction of fluorescence intensity at 343 nm, data not shown).

Upon coelenterazine binding, tryptophan fluorescence of apo-obelin is quenched [14]. Bound 2-hydroperoxycoelenterazine is weakly fluorescent (Fig. 3A, black line), whereas bound coelenteramide is highly fluorescent with an emission maximum around 500 nm upon excitation at 295 nm (Fig. 3B and C, black lines). The green fluorescence of coelenteramide bound to obelin is mainly due to Förster resonance energy transfer from tryptophans. This is concluded from the observed quenching of tryptophan fluorescence of obelin upon binding of coelenteramide (Fig. 3C, left panel).

We also studied reversibility of thermal unfolding of active obelin (II) and Ca^{2+}-discharged obelins, both with and without calcium (III and IV), by using fluorescence spectroscopy. Samples are heated to 80 °C and subsequently cooled to 20 °C and display no visible turbidity. Tryptophan fluorescence of these obelin conformational states increases after this heating procedure (Fig. 3, left panels).

In case of active obelin (II), a strong increase of fluorescence occurs at 420 and 500 nm (Fig. 3A, left panel) that might be attributed to heat-induced, calcium-independent oxidation of 2-hydroperoxycoelenterazine yielding bound coelenteramide (500 nm) [18] and probably some side-product (420 nm) [19] or to an obelin conformational state that assists in the formation of exited coelenteramide in its neutral state [20]. In case of Ca^{2+}-discharged obelin with coelenteramide bound (IV) the heating procedure causes a decrease in fluorescence at 500 nm (Fig. 3B, left panel). This fluorescence completely vanishes in case of Ca^{2+}-discharged obelin with both coelenteramide and calcium bound (III)

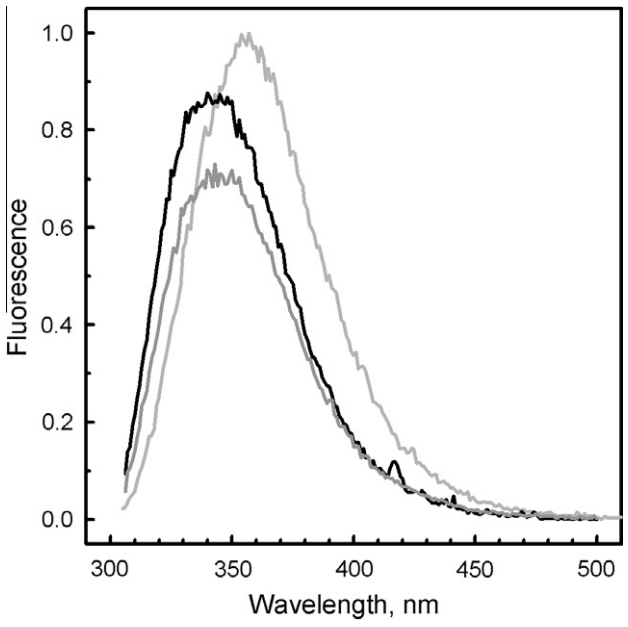

Fig. 2. Reversibility of thermal unfolding of apo-obelin (I). Normalized fluorescence emission spectra of apo-obelin are shown before thermal unfolding (black line), after increasing temperature up to 80 °C and subsequent cooling down (dark gray line), and of apo-obelin in 6.0 M GuHCl (light gray line). Excitation is at 295 nm and temperature is 20 °C.

(Fig. 3C, left panel). Because free coelenteramide is non-fluorescent in solution, these observations suggest that coelenteramide dissociates from obelin during heating and that in presence of calcium this dissociation is irreversible.

The various ligand-dependent conformational states of obelin differ significantly in stability against thermal unfolding (Fig. 4). Both apo-obelin forms (I and V) have thermal unfolding curves that display no distinct midpoints of unfolding (Fig. 4A). These curves show highly non-cooperative unfolding behavior, suggesting that apo-obelin is an ensemble of multiple conformational states, the populations of which alter upon increasing temperature. In case of calcium-loaded apo-obelin (V), the unfolding curve shifts to slightly higher temperature (Fig. 4A).

Thermal unfolding of active obelin (II) is highly cooperative (Fig. 4A), which suggests that active obelin is in a single conformational state. Fitting of a two-state unfolding model to the thermal unfolding data of state II shows that its thermal midpoint of unfolding (T_m) is 52.1 ± 0.1 °C (Fig. 4A). Active obelin containing 2-hydroperoxycoelenterazine is thus a relatively stable protein. Upon thermal unfolding of active obelin, its tryptophan fluorescence significantly increases (Figs. 3A (left panel) and 4A), because 2-hydroperoxycoelenterazine is no longer bound and thus does not quench fluorescence.

Ca^{2+}-discharged obelin with both coelenteramide and calcium bound (III) has a thermal unfolding curve with a midpoint of unfolding of 54.5 ± 0.2 °C (Fig. 4B), i.e., similar to the value that characterizes active obelin. However, the curvature of the native baseline part of this unfolding curve suggests that Ca^{2+}-discharged obelin with both coelenteramide and calcium bound comprises some interconverting conformational states. Removal of calcium and thus generating state IV decreases protein stability considerably, because now T_m becomes 31.4 ± 1.0 °C (Fig. 4B).

The protein conformations of which thermal midpoints could be determined (II, III and IV) were heated to their respective T_m-values and subsequently cooled down to 20 °C (Fig. 3, right panels). This procedure does not alter fluorescence of obelin states III and IV (Fig. 3B and C, right panels). It shows that both obelin states are capable of reversibly binding coelenteramide up to their respective T_m-values. At higher temperatures, however, both conformations lose their coelenteramide binding capacity (Fig. 3). In case of active obelin (II), applying the mentioned heating procedure leads to strong fluorescence at 500 nm (Fig. 3A, right panel). This clearly shows that for state II irreversible processes happen at T_m, which is due to conversion of 2-hydroperoxycoelenterazine into coelenteramide as a result of Ca^{2+}-independent light emission upon heating. Midpoints of thermal unfolding are summarized in Table 1.

3.2. Thermal unfolding of obelin studied by far-UV CD

Far-UV CD spectra of ligand-dependent obelin conformations are typical for those of helical proteins, and thus these spectra have ellipticity minima at 208–210 nm and 222 nm (Fig. 5). Active obelin (II) shows the highest helical content. Far-UV CD spectra of Ca^{2+}-discharged forms of obelin (containing both coelenteramide and calcium (III) or containing only coelenteramide (IV)) are virtually indistinguishable. Both spectra display less negative ellipticities as compared to the far-UV CD spectrum of state II. Calcium-loaded apo-obelin (V) has the lowest helical content of all obelin conformations containing ligands, because it has the lowest ellipticity at 220 nm. Apo-obelin (I) is structurally distinct from the other obelin states, because its far-UV CD spectrum has a zero crossing at 202.5 nm, whereas the other obelin conformational states have their zero crossing around 204 nm (Fig. 5).

Thermal unfolding of ligand-dependent obelin conformations causes significant changes in ellipticities at 220 nm (Fig. 6). Fitting of a two-state unfolding model to these data gives T_m-values of

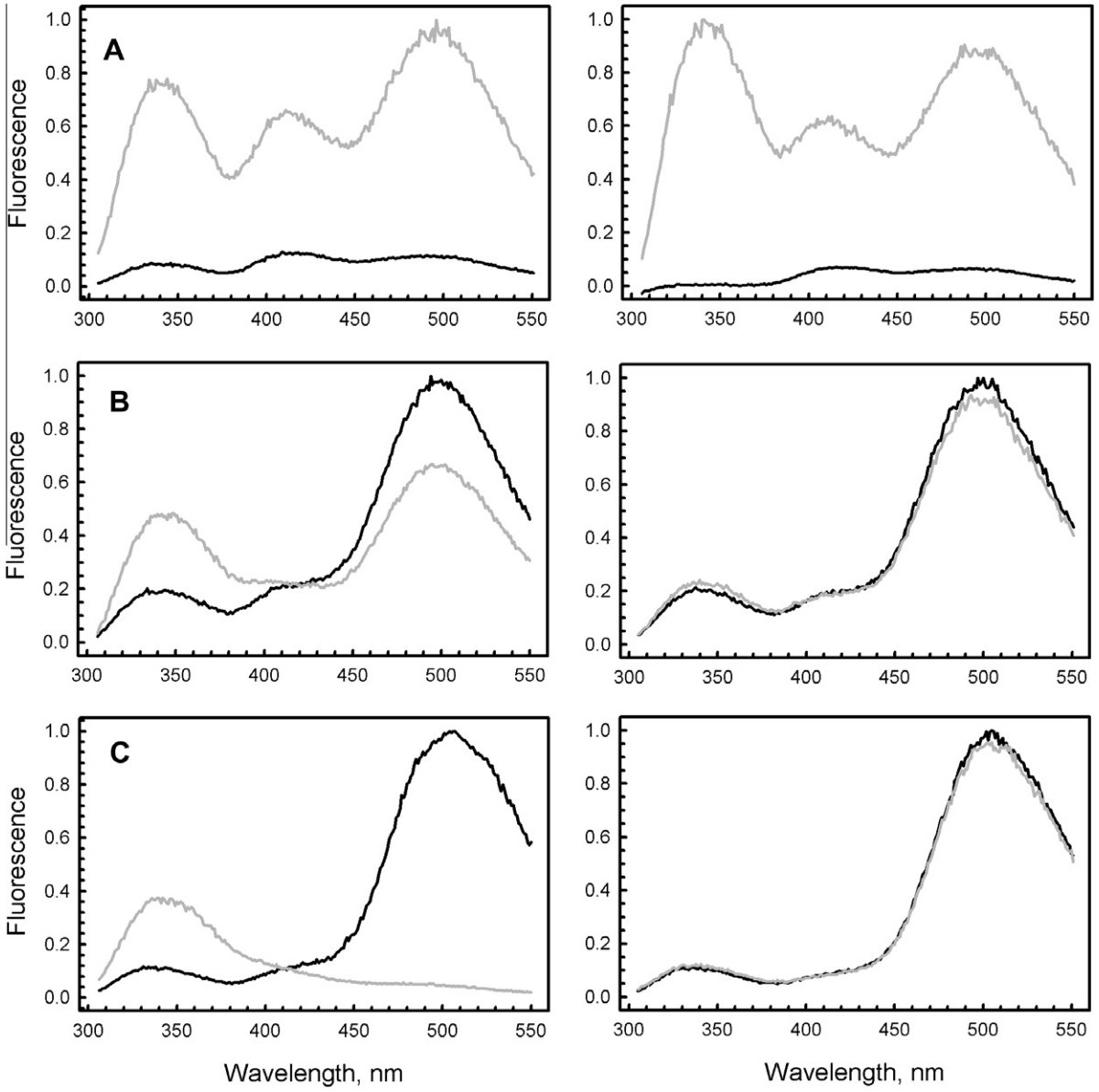

Fig. 3. Fluorescence of ligand-dependent conformations of obelin. Left panels show spectra of protein before (black line) and after thermal unfolding by increasing temperature to 80 °C and subsequent cooling to 20 °C (gray line). Right panels show spectra of protein before (black line) and after heating to their midpoints of thermal unfolding (i.e., 52, 31, and 54 °C, respectively) and subsequent cooling to 20 °C. (A) active obelin containing 2-hydroperoxycoelenterazine (II); (B) Ca^{2+}-discharged obelin containing coelenteramide (IV); (C) Ca^{2+}-discharged obelin containing both coelenteramide and calcium (III). Excitation is at 295 nm and temperature is 20 °C.

34.5 ± 1.2 °C for apo-obelin (I), 42.5 ± 0.3 °C for apo-obelin loaded with calcium (V), 54.8 ± 0.2 °C for active obelin (II), 78.2 ± 0.3 °C for Ca^{2+}-discharged obelin containing coelenteramide and Ca^{2+} (III), and 37.1 ± 0.5 °C for Ca^{2+}-discharged obelin containing only coelenteramide (IV) (Table 1). It should be noted that, according to far-UV CD spectra of ligand-dependent obelin conformations before and after thermal unfolding at 80 °C and subsequent cooling to 20 °C, the temperature-induced unfolding of all these conformations is not fully reversible (Fig. 7).

4. Discussion

X-ray crystallography yielded spatial structures for four of five ligand-dependent obelin conformations (Fig. 1). These structures have the same compact two-domain fold, which consists of four sets of helix-turn-helix structural motifs specific for EF-hand calcium-binding domains [21]. The coelenterazine-binding pocket of obelin is highly hydrophobic and is formed by residues originating from all eight helices. In addition, several hydrophilic side chains are directed into this pocket. Upon going from substrate-containing obelin state II to product-containing obelin state IV, the largest structural change observed concerns the position of the key amino acid residues in the reaction center around the C2-carbon of coelenterazine [22].

Both N- and C-termini of calcium-loaded apo-obelin are not observed in the electron density map of the protein, because of their flexibility. In contrast, the C-terminus caps the substrate-binding cavity containing 2-hydroperoxycoelenterazine in active obelin (II) and the ligand cavity containing coelenteramide in Ca^{2+}-discharged obelin (III), which results in its solvent-inaccessibility and, therefore, in non-polar environment of substrate or product.

In the calcium-loaded forms of Ca^{2+}-discharged obelin and apo-obelin (III and V, respectively) 12 residues of the EF-hand calcium-binding loops I, III, and IV shift their relative positions [23]. Among

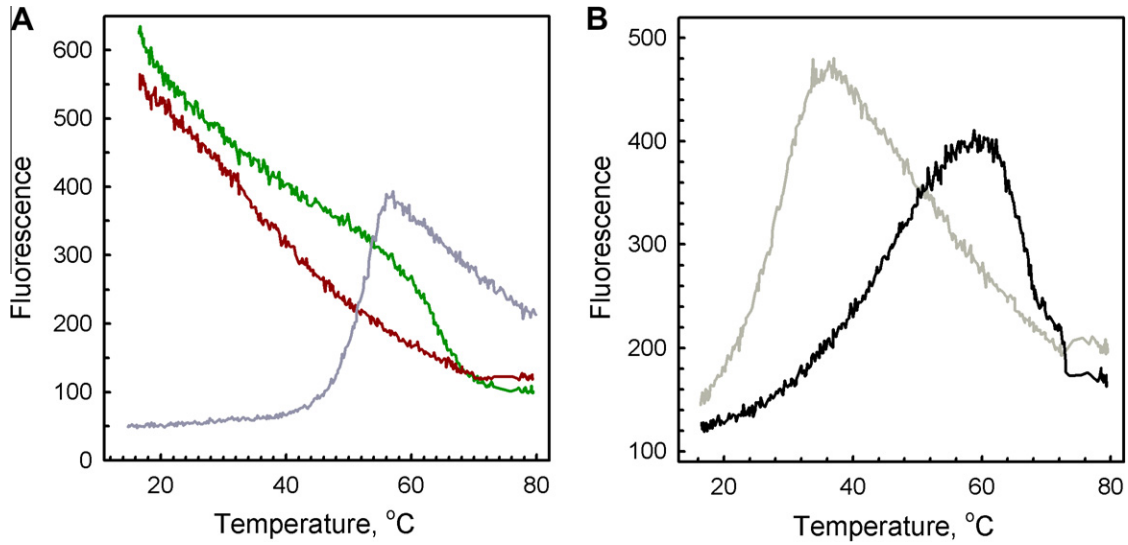

Fig. 4. Thermal unfolding of ligand-dependent obelin conformations followed by fluorescence spectroscopy. Shown are changes in fluorescence emission at 340 nm. A, apo-obelin (I) (dark red line), calcium-loaded apo-obelin (V) (dark green line) and active obelin (II) (dark gray line); B, Ca^{2+}-discharged obelin containing both coelenteramide and calcium (III) (black line) and Ca^{2+}-discharged obelin containing only coelenteramide (IV) (light gray line).

Table 1
Midpoints of thermal unfolding of ligand-dependent obelin conformations, derived from changes in fluorescence emission at 340 nm and ellipticity at 220 nm.

Obelin state	T_m via fluorescence at 340 nm (°C)	T_m via CD at 220 nm (°C)
Apo-obelin, no Ca^{2+} (I)	n.d.[a]	34.5 ± 1.2
Apo-obelin, Ca^{2+} (V)	n.d.[a]	42.5 ± 0.3
Active obelin, no Ca^{2+} (II)	52.1 ± 0.1	54.8 ± 0.2
Discharged obelin, Ca^{2+} (III)	54.5 ± 0.2	78.2 ± 0.3
Discharged obelin, no Ca^{2+} (IV)	31.4 ± 1.0	37.1 ± 0.5

[a] Not determinable.

these loops, loop IV undergoes the largest change in terms of residue reorientation and repositioning. In addition, calcium binding to active obelin results in a reorganization of the protein's hydrogen-bond network [23]. However, overall inspection of the crystal structures shows that calcium binding to obelin does not result in large changes in protein conformation. This observation suggests that Ca^{2+}-regulated photoproteins are calcium-signal modulators (like for example parvalbumin) rather than being calcium-sensors (like for example calmodulin) [24].

The fluorescence and far-UV CD data reported in this study show that coelenterazine binding considerably stabilizes obelin against thermal unfolding. Whereas apo-obelin (I) shows non-cooperative temperature-induced unfolding behavior detected by fluorescence spectroscopy, active obelin containing 2-hydroperoxycoelenterazine (II) has a distinct unfolding transition at 52.1 ± 0.1 °C (Table 1). Calcium binding also stabilizes apo-obelin against thermal unfolding, as fluorescence spectroscopy shows (Fig. 4A), and according to far-UV CD spectroscopy (Fig. 6A) the thermal midpoint of secondary structure unfolding increases by 8 °C (Table 1).

Whereas unfolding experiments using fluorescence predominantly report about changes in tryptophan microenvironments, reflecting distortion of tertiary structure, far-UV CD reports about alterations in protein secondary structure. In case of Ca^{2+}-discharged obelin containing coelenteramide and calcium (III), fluorescence and far-UV CD spectroscopy report midpoints of

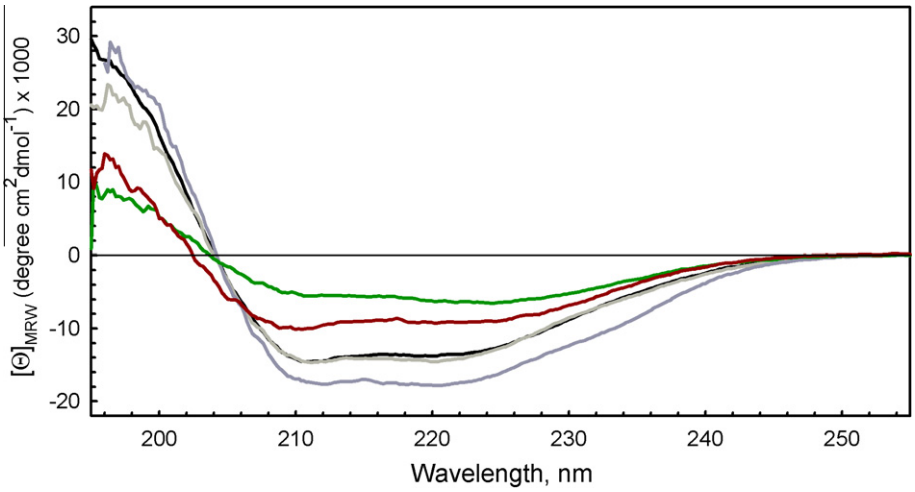

Fig. 5. Far-UV CD spectra of ligand-dependent obelin conformations. Spectra are of apo-obelin (I) (dark red line), calcium loaded apo-obelin (V) (dark green line), active obelin (II) (dark gray line), Ca^{2+}-discharged obelin containing both coelenteramide and calcium (III) (black line) and Ca^{2+}-discharged obelin containing only coelenteramide (IV) (light gray line). Protein concentration is 4 μM in 5 mM Tris–HCl, pH 7.0, with addition of either 1 mM EDTA or 1 mM $CaCl_2$. Temperature is 20 °C.

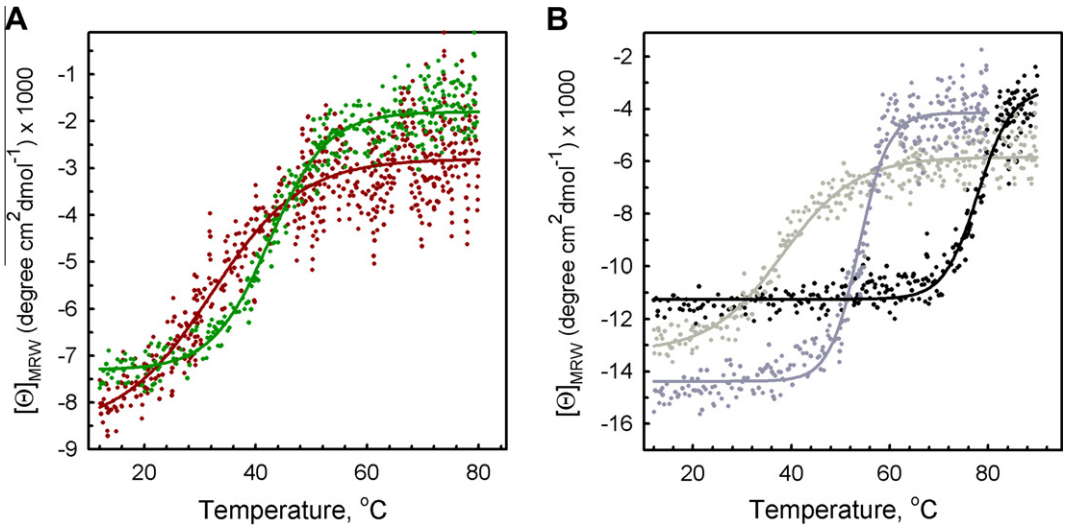

Fig. 6. Thermal unfolding of ligand-dependent obelin conformations followed by far-UV CD. Shown are changes in ellipticities at 220 nm. (A) Apo-obelin (I) (dark red line), calcium-loaded apo-obelin (V) (dark green line); (B) active obelin (II) (dark gray line), Ca^{2+}-discharged obelin containing both coelenteramide and calcium (III) (black line) and Ca^{2+}-discharged obelin containing only coelenteramide (V) (light gray line). Protein concentration is 4 μM in 25 mM HEPES, pH 7.0 with addition of either 1 mM EDTA or 1 mM $CaCl_2$.

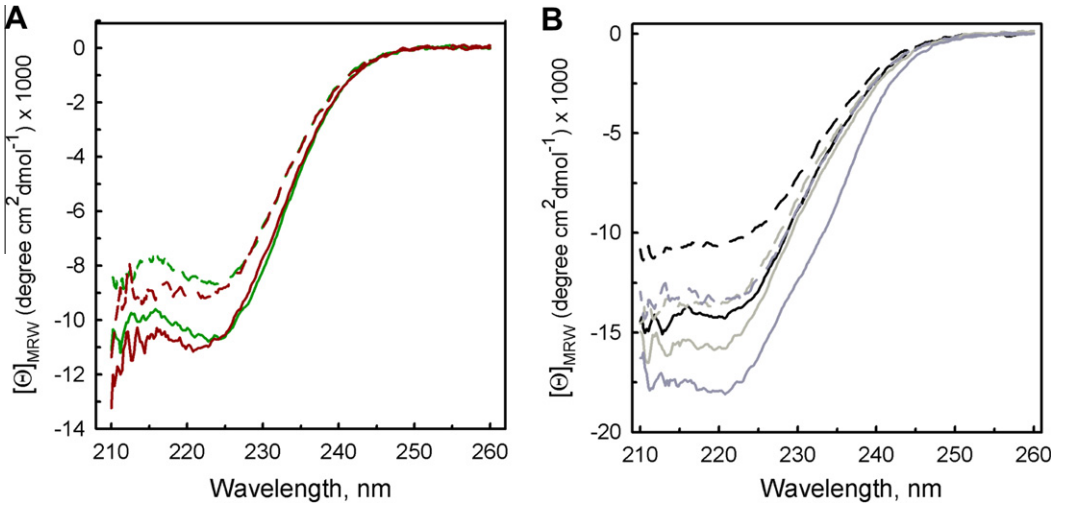

Fig. 7. Far-UV CD spectra of ligand-dependent obelin conformations before (solid line) and after thermal unfolding at 80 °C (dashed line). (A) Apo-obelin (I) (dark red line), calcium-loaded apo-obelin (V) (dark green line); (B) active obelin (II) (dark gray line), Ca^{2+}-discharged obelin containing both coelenteramide and calcium (III) (black line) and Ca^{2+}-discharged obelin containing only coelenteramide (IV) (light gray line). Protein concentration is 4 μM in 25 mM HEPES, pH 7.0, with addition of either 1 mM EDTA or 1 mM $CaCl_2$. Temperature is 20 °C.

thermal unfolding differing by 23.7 °C (Table 1). Upon thermal unfolding of Ca^{2+}-discharged obelin (III), tertiary side-chain packing involving tryptophans is apparently lost before protein secondary structure is disrupted. This phenomenon is typical for formation of molten globules, which are ensembles of interconverting protein conformers that have a substantial amount of secondary structure, but lack virtually all tertiary side-chain packing of natively folded proteins. In this molten globule, calcium possibly remains bound to the EF-hand Ca^{2+}-binding loops I, III, and IV, which do not contain tryptophans [23]. Far-UV CD would report the structuring of these protein regions, whereas it would remain undetected by tryptophan fluorescence, which reports the unfolding behavior of other parts of the protein.

This study shows that calcium-loaded apo-obelin (V) has a rather low helical content as it has a low ellipticity at 220 nm (Fig. 5). This observation differs from the one obtained from crystallography, which shows that this state has 101 out of 195 residues involved in helices compared to 115 helical residues in case of active obelin [23]. However, as thermal unfolding monitored by fluorescence shows (Fig. 4), in solution calcium-loaded apo-obelin (V) is an ensemble of conformational states, which apparently involves less structured ones as well. Apo-obelin (I) is also an ensemble of conformational states. It differs structurally from the other obelin states, because its far-UV CD spectrum has a zero crossing at 202.5 nm, whereas the other obelin conformational states have their zero crossing at 204 nm (Fig. 5). These characteristics of apo-obelin (I) possibly prevented its crystallization to date.

Acknowledgements

The work was supported by RFBR grant 12-04-00131, by the Program of the Government of Russian Federation "Measures to Attract Leading Scientists to Russian Educational Institutions" (grant 11.G34.31.058), by the Program "Molecular and Cellular

Biology" of RAS. The Wageningen University Sandwich PhD-Fellowship Program supported E.V.E.

References

[1] Fisher, W.R., Taniuchi, H. and Anfinsen, C.B. (1973) On the role of heme in the formation of the structure of cytochrome c. J. Biol. Chem. 248, 3188–3195.

[2] Steensma, E., Nijman, M.J.M., Bollen, Y.J.M., de Jager, P.A., van den Berg, W.A.M., van Dongen, W.M.A.M. and van Mierlo, C.P.M. (1998) Apparent local stability of the secondary structure of *Azotobacter vinelandii* holoflavodoxin II as probed by hydrogen exchange: implications for redox potential regulation and flavodoxin folding. Protein Sci. 7, 306–317.

[3] Steensma, E. and van Mierlo, C.P.M. (1998) Structural characterisation of apoflavodoxin shows that the location of the stable nucleus differs among proteins with a flavodoxin-like topology. J. Mol. Biol. 282, 653–666.

[4] Bollen, Y.J., Westphal, A.H., Lindhoud, S., van Berkel, W.J.H. and van Mierlo, C.P.M. (2012) Distant residues mediate picomolar-binding affinity of a protein cofactor. Nat. Commun., http://dx.doi.org/10.1038/ncomms2010.

[5] Shimomura, O. (2006) Bioluminescence: Chemical Principles and Methods, World Scientific Publishing, Singapore.

[6] Shimomura, O. and Johnson, F.H. (1975) Regeneration of the photoprotein aequorin. Nature 256, 236–238.

[7] Shimomura, O. and Johnson, F.H. (1972) Structure of the light-emitting moiety of aequorin. Biochemistry 11, 1602–1608.

[8] Vysotski, E.S. and Lee, J. (2004) Ca^{2+}-regulated photoproteins: structural insight into the bioluminescence mechanism. Acc. Chem. Res. 37, 405–415.

[9] Allen, D.G., Blinks, J.R. and Prendergast, F.G. (1977) Aequorin luminescence: relation of light emission to calcium concentration—a calcium-independent component. Science 195, 996–998.

[10] Lee, J., Glushka, J.N., Markova, S.V. and Vysotski, E.S. (2001) Protein conformational changes in obelin shown by ^{15}N-HSQC nuclear magnetic resonance in: Bioluminescence and Chemiluminescence (Case, J.F., Herring, B.H., Robison, B.H., Haddock, S.H.D., Kricka, L.J. and Stanley, P.E., Eds.), pp. 99–102, World Scientific Publishing Co., Singapore.

[11] Liu, Z.J., Stepanyuk, G.A., Vysotski, E.S., Lee, J., Markova, S.V., Malikova, N.P. and Wang, B.C. (2006) Crystal structure of obelin after Ca^{2+}-triggered bioluminescence suggests neutral coelenteramide as the primary excited state. Proc. Natl. Acad. Sci. USA 103, 2570–2575.

[12] Illarionov, B.A., Frank, L.A., Illarionova, V.A., Bondar, V.S., Vysotski, E.S. and Blinks, J.R. (2000) Recombinant obelin: cloning and expression of cDNA purification, and characterization as a calcium indicator. Methods Enzymol. 305, 223–249.

[13] Vysotski, E.S., Liu, Z.J., Rose, J., Wang, B.C. and Lee, J. (2001) Preparation and X-ray crystallographic analysis of recombinant obelin crystals diffracting to beyond 1.1 Å. Acta Crystallogr. D: Biol. Crystallogr. 57, 1919–1921.

[14] Eremeeva, E.V., Markova, S.V., Westphal, A.H., Visser, A.J., van Berkel, W.J. and Vysotski, E.S. (2009) The intrinsic fluorescence of apo-obelin and apo-aequorin and use of its quenching to characterize coelenterazine binding. FEBS Lett. 583, 1939–1944.

[15] Pace, C.N. and Laurents, D.V. (1989) A new method for determining the heat capacity change for protein folding. Biochemistry 28, 2520–2525.

[16] Becktel, W.J. and Schellman, J.A. (1987) Protein stability curves. Biopolymers 26, 1859–1877.

[17] Privalov, P.L. and Khechinashvili, N.N. (1974) A thermodynamic approach to the problem of stabilization of globular protein structure: a calorimetric study. J. Mol. Biol. 86, 665–684.

[18] Ray, B.D., Ho, S., Kemple, M.D., Prendergast, F.G. and Nageswara Rao, B.D. (1985) Proton NMR of aequorin. Structural changes concomitant with calcium-independent light emission. Biochemistry 24, 4280–4287.

[19] Shimomura, O. and Teranishi, K. (1973) Chemical nature of light emitter in bioluminescence of aequorin. Tetrahedron Lett., 2963–2966.

[20] Shimomura, O. and Teranishi, K. (2000) Light-emitters involved in the luminescence of coelenterazine. Luminescence 15, 51–58.

[21] Liu, Z.J., Vysotski, E.S., Chen, C.J., Rose, J.P., Lee, J. and Wang, B.C. (2000) Structure of the Ca^{2+}-regulated photoprotein obelin at 1.7 Å resolution determined directly from its sulfur substructure. Protein Sci. 11, 2085–2093.

[22] Deng, L., Markova, S.V., Vysotski, E.S., Liu, Z.J., Lee, J., Rose, J. and Wang, B.C. (2004) Crystal structure of a Ca^{2+}-discharged photoprotein: implications for mechanisms of the calcium trigger and bioluminescence. J. Biol. Chem. 279, 33647–33652.

[23] Deng, L., Vysotski, E.S., Markova, S.V., Liu, Z.J., Lee, J., Rose, J. and Wang, B.C. (2005) All three Ca^{2+}-binding loops of photoproteins bind calcium ions: the crystal structures of calcium-loaded apo-aequorin and apo-obelin. Protein Sci. 14, 663–675.

[24] Nelson, M.R. and Chazin, W.J. (1998) Structures of EF-hand Ca(2+)-binding proteins: diversity in the organization, packing and response to Ca^{2+} binding. Biometals 11, 297–318.